Supporting information for: Structural and dynamical characterization of DNA and RNA quadruplex obtained from the GGGGCC hexanucleotide repeats that are the hallmark of C9FTD/ALS diseases

Yuan Zhang, Christopher Roland, and Celeste Sagui*

Department of Physics, North Carolina State University, Raleigh, NC 27695

E-mail: sagui@ncsu.edu,Ph:(919)515-3111

1 Analysis

1.1 Quadruplex twist

The twist angle of G-quadruplex models is the angle between two vectors defined as follows: one vector joins the C1' atoms of two adjacent bases on the same layer, and the other one is the corresponding vector on the next layer. Rather than using this angle directly, we use the projection onto the plane perpendicular to the global helical axis U. This axis is defined as the mean vector of U1, U2, U3, and U4, each of which links the C1' atoms of the nucleotides of the current G-layer and the next G-layer in the corresponding strand of the quadruplex. The base rotations are positive for a right-hand rotation around the 5'-3' direction.

---

[*] To whom correspondence should be addressed

1.2 Quadruplex buckle displacement

While the buckle displacement in a duplex involves two bases in a basepair, the buckle displacement in a quadruplex involves 4 bases on the same layer in order to quantify the out-of-plane deviations of the quartet. It is defined as the relative positions of the centers of mass of two tetragons: the outer tetragon is formed by N9 atoms and the inner one is formed by O6 atoms, as shown in Fig.S2.

1.3 Ion position through the inner interbase channel

We first define the channel axis as the mean vector of U1, U2, U3, and U4, each of which links the O6 atoms of the nucleotides of the 1st G-layer and 4th G-layer in the corresponding strand of the quadruplex. The center of mass of O6 atoms on the first layer is defined as the origin. The distance between ion and axis has been calculated and if it is smaller than a cutoff (5.0 Å), it is treated as in the channel. The position of the ion diffusing into the channel has been recorded as the projection position on the axis.

2 Results

The following figures, cited in the main text, further illustrate and support points explained in the main text.

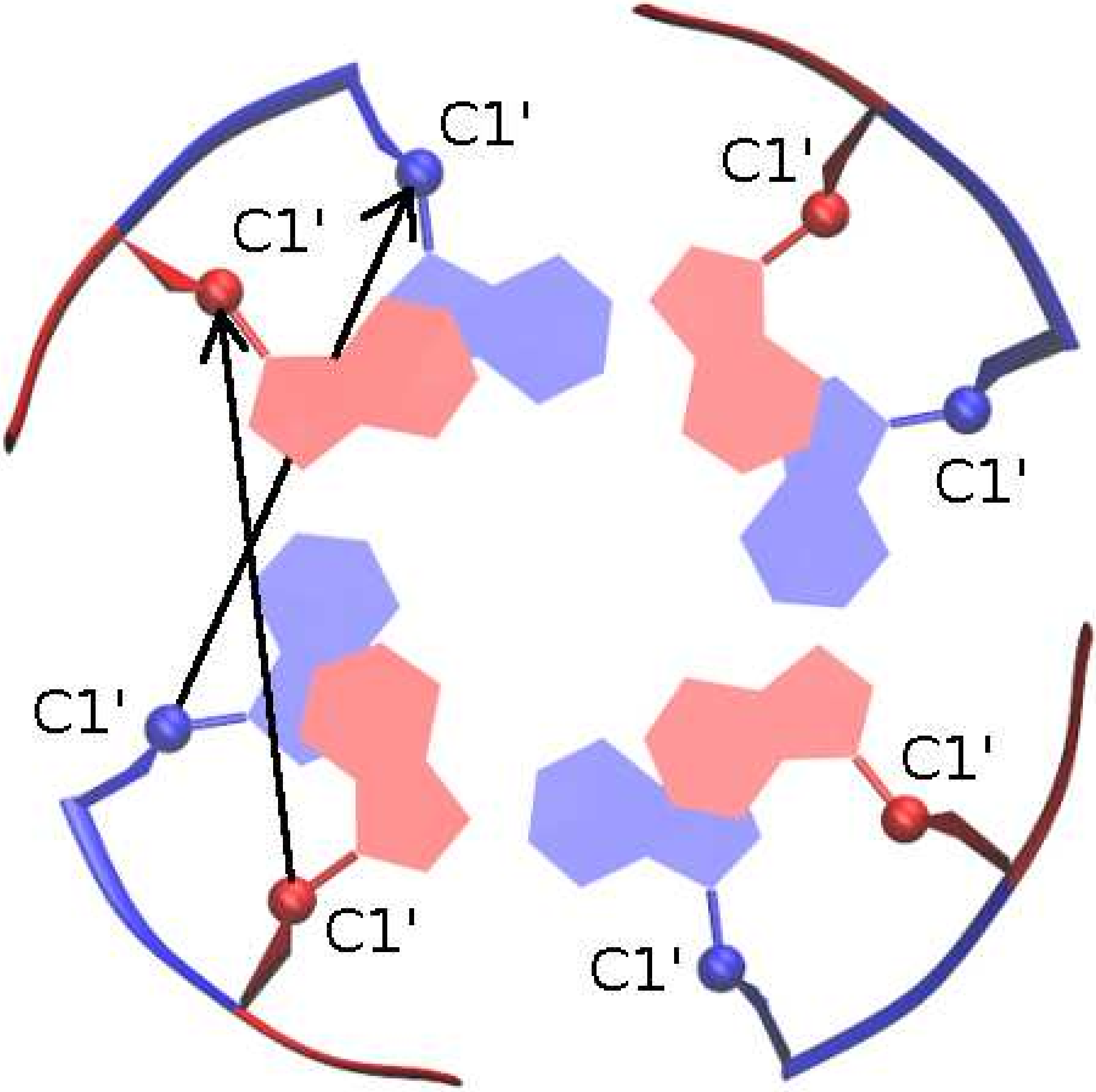

Figure S1: Definition of quadruplex twist angle.

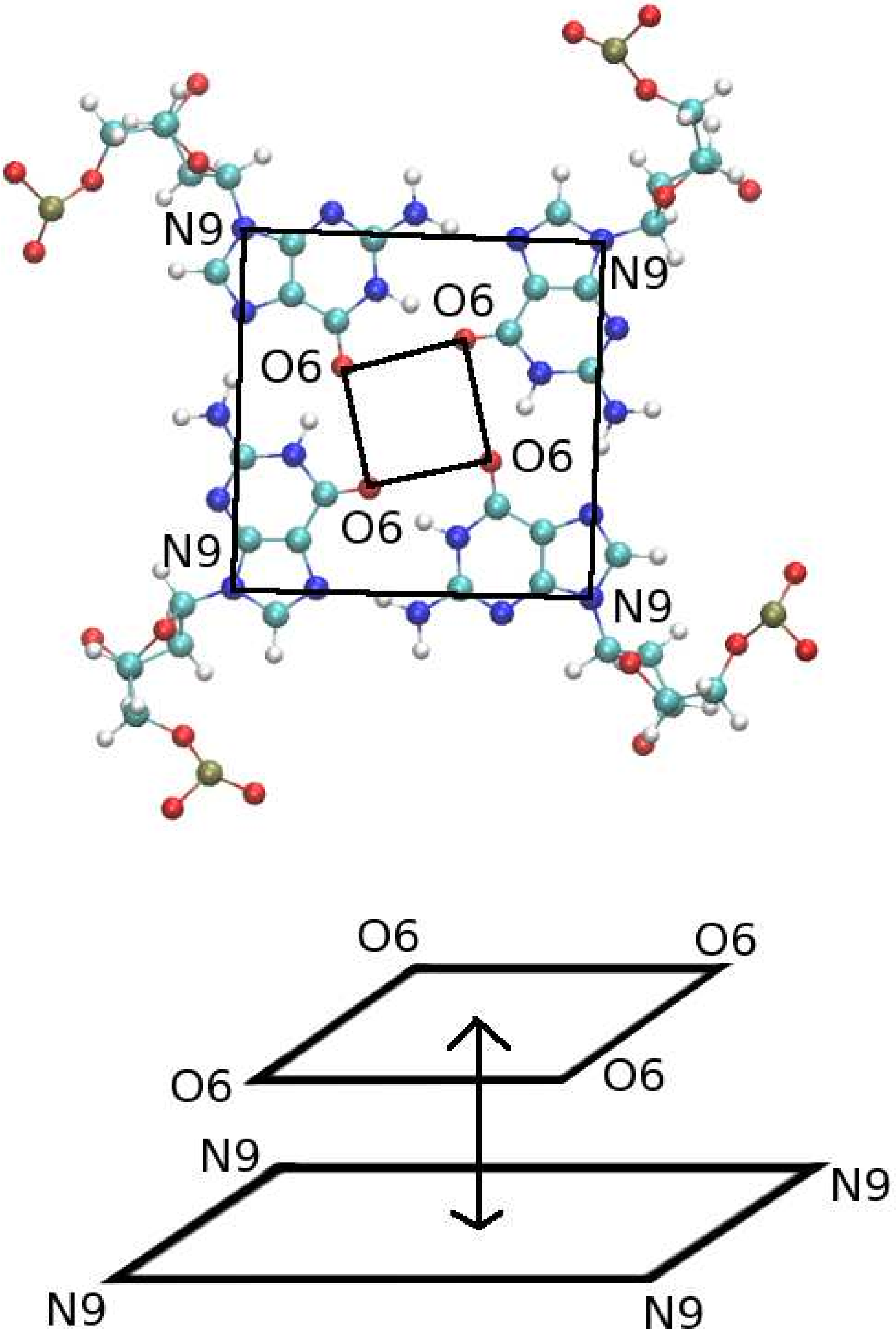

Figure S2: Definition of quadruplex buckle displacement.

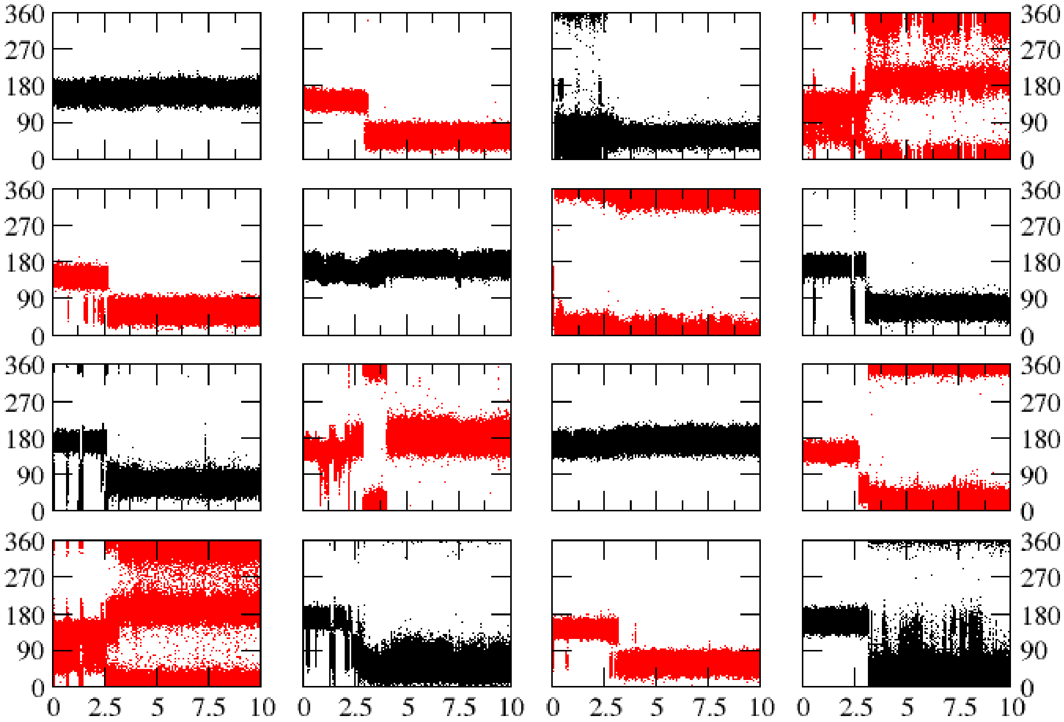

Figure S3: Pseudorotation phase angle of all the G bases in RNA AQ-1 as a function of time. The G_{anti} bases are depicted red, and the G_{syn} bases are black. Each row shows the bases within the same G-quartet plane.

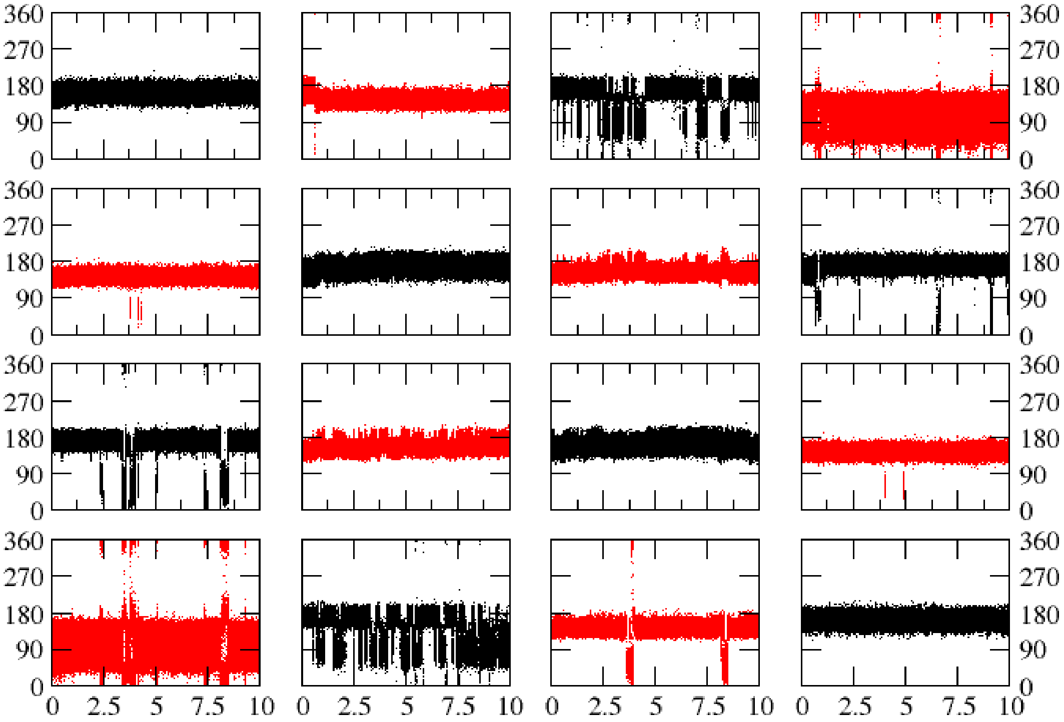

Figure S4: Pseudorotation phase angle of all the G bases in RNA AQ-1-L as a function of time. The G_{anti} bases are depicted red, and the G_{syn} bases are black. Each row shows the bases within the same G-quartet plane.

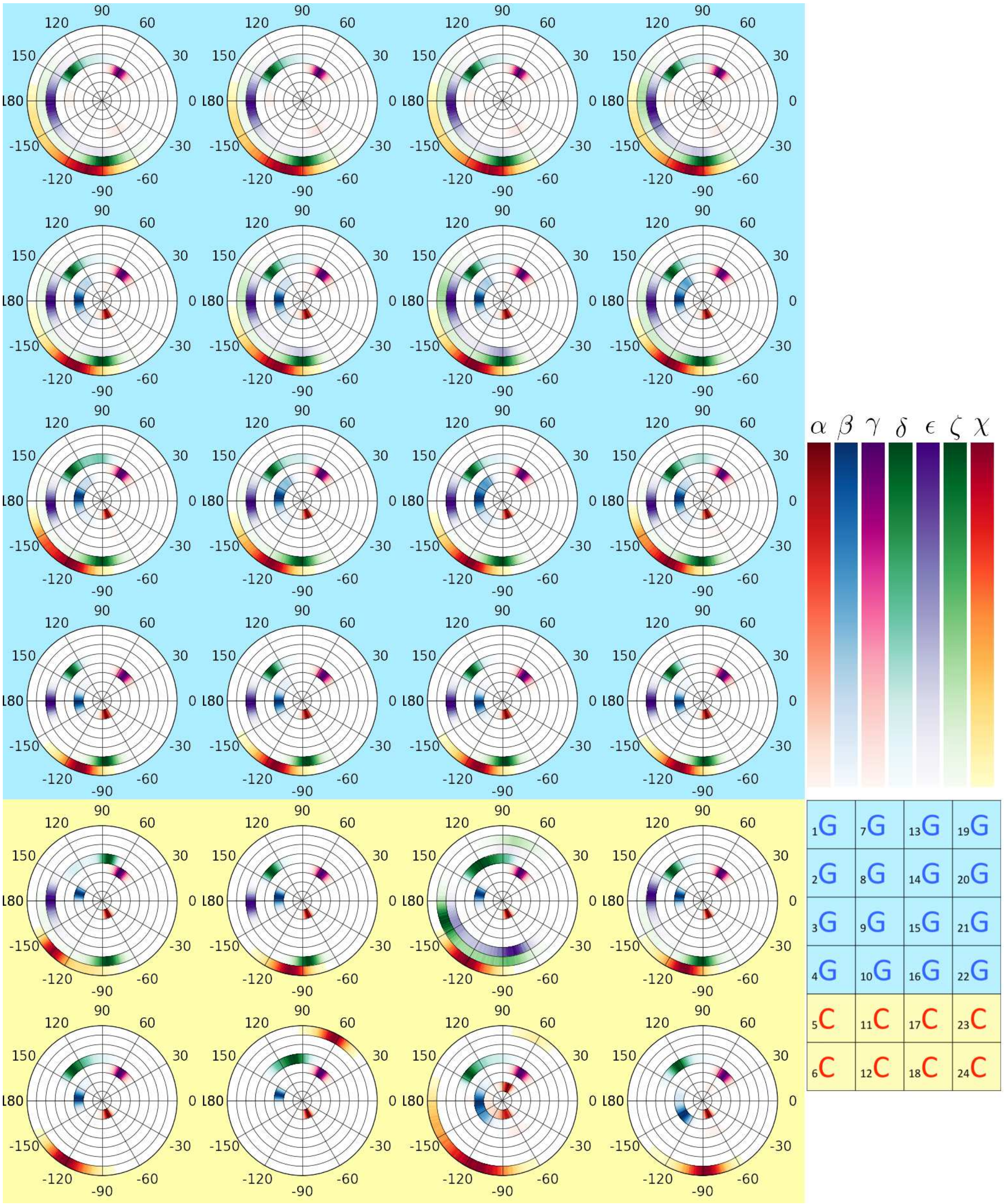

Figure S5: Torsion angle density distribution (α, β, γ, δ, ϵ, ζ, χ, from inner to outer circle ring) for each base in DNA PQ during the last 500 ns of the simulation. G-layers are shown in blue and C-layers in yellow. G bases on the same layer are shown in the same row, according to the map on the right.

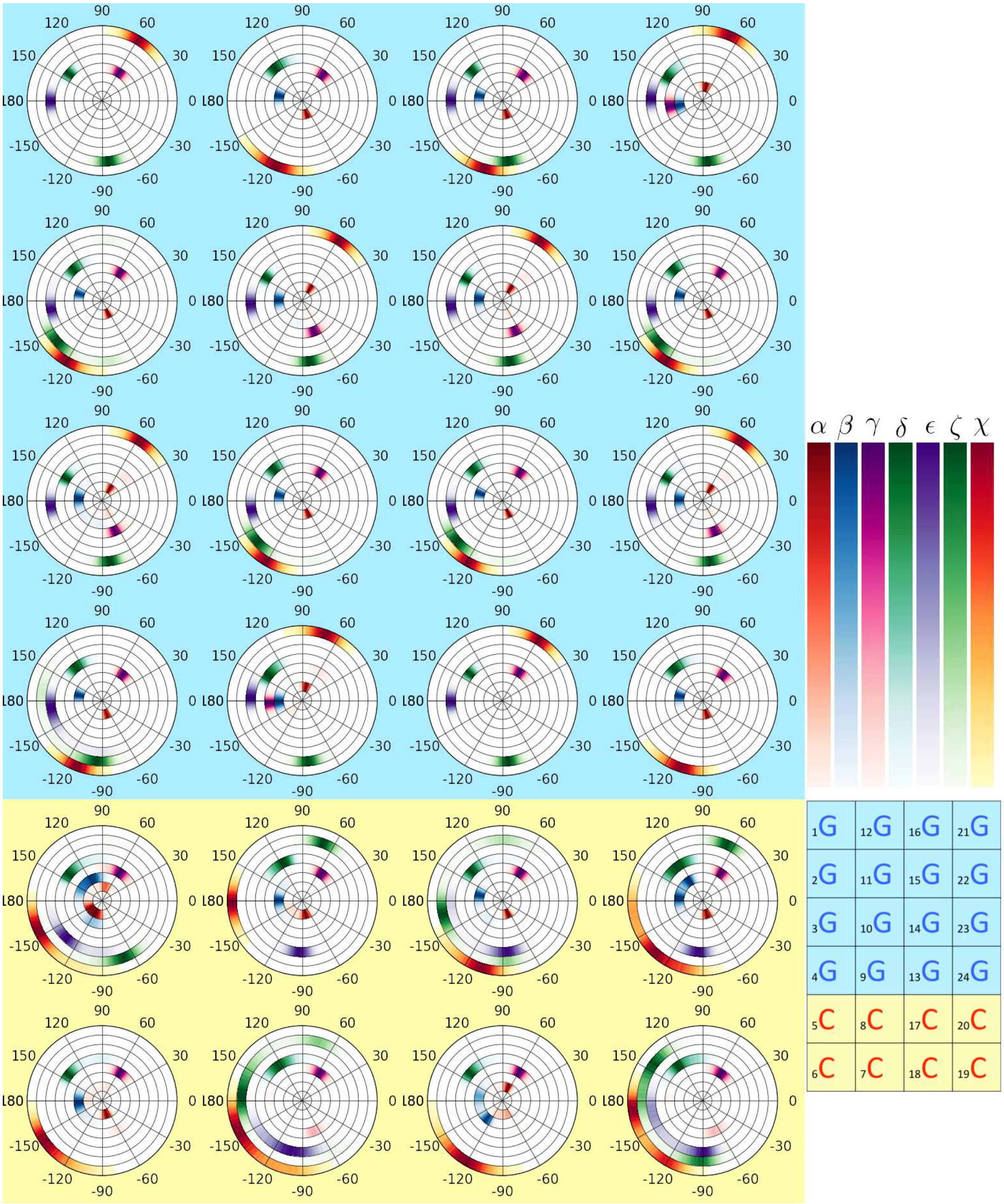

Figure S6: Torsion angle density distribution (α, β, γ, δ, ϵ, ζ, χ, from inner to outer circle ring) for each base in DNA AQ-1 during the last 500 ns of the simulation. G-layers are shown in blue and C-layers in yellow. G bases on the same layer are shown in the same row, according to the map on the right.

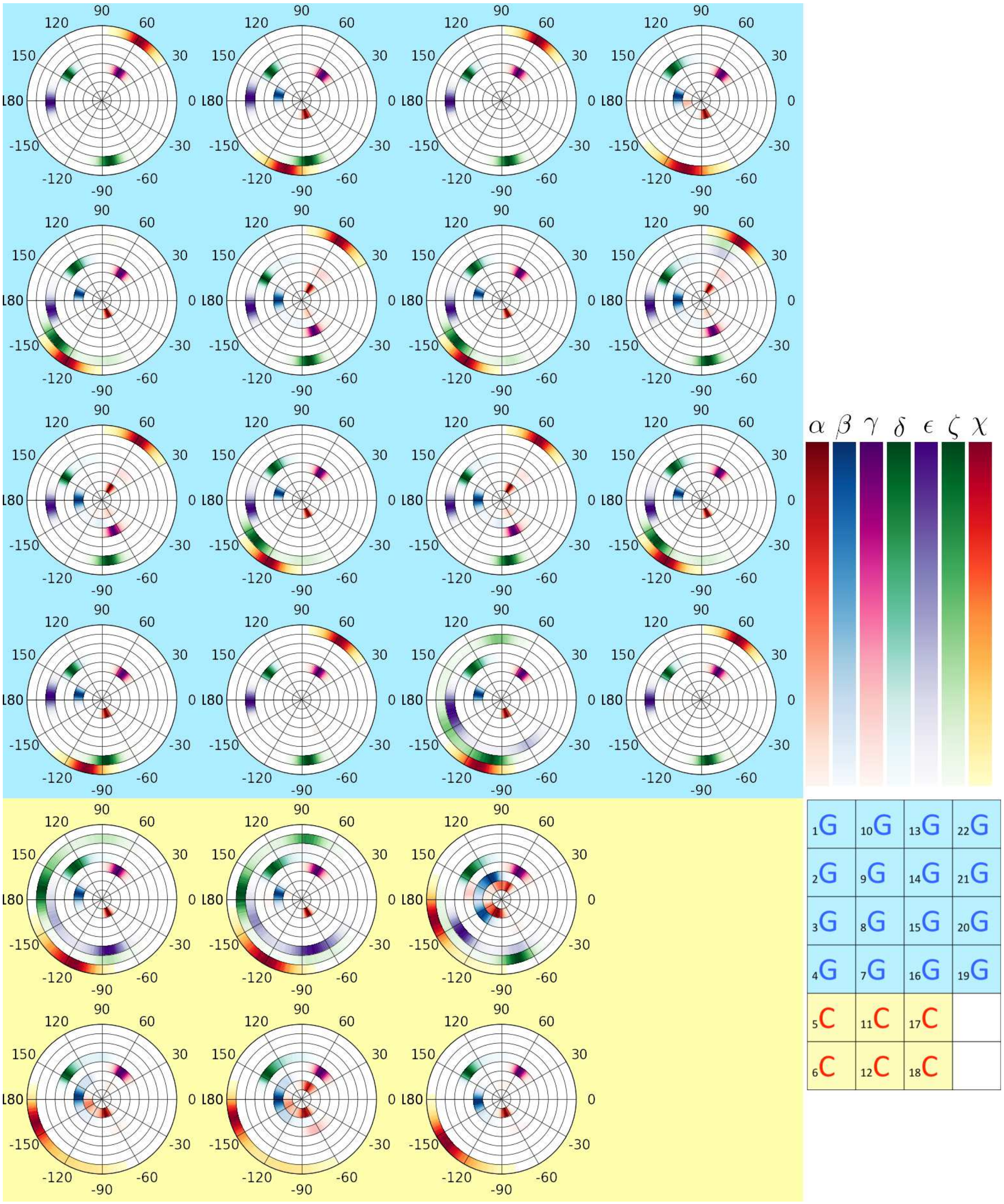

Figure S7: Torsion angle density distribution (α, β, γ, δ, ϵ, ζ, χ, from inner to outer circle ring) for each base in DNA AQ-2 during the last 500 ns of the simulation. G-layers are shown in blue and C-layers in yellow. G bases on the same layer are shown in the same row, according to the map on the right.

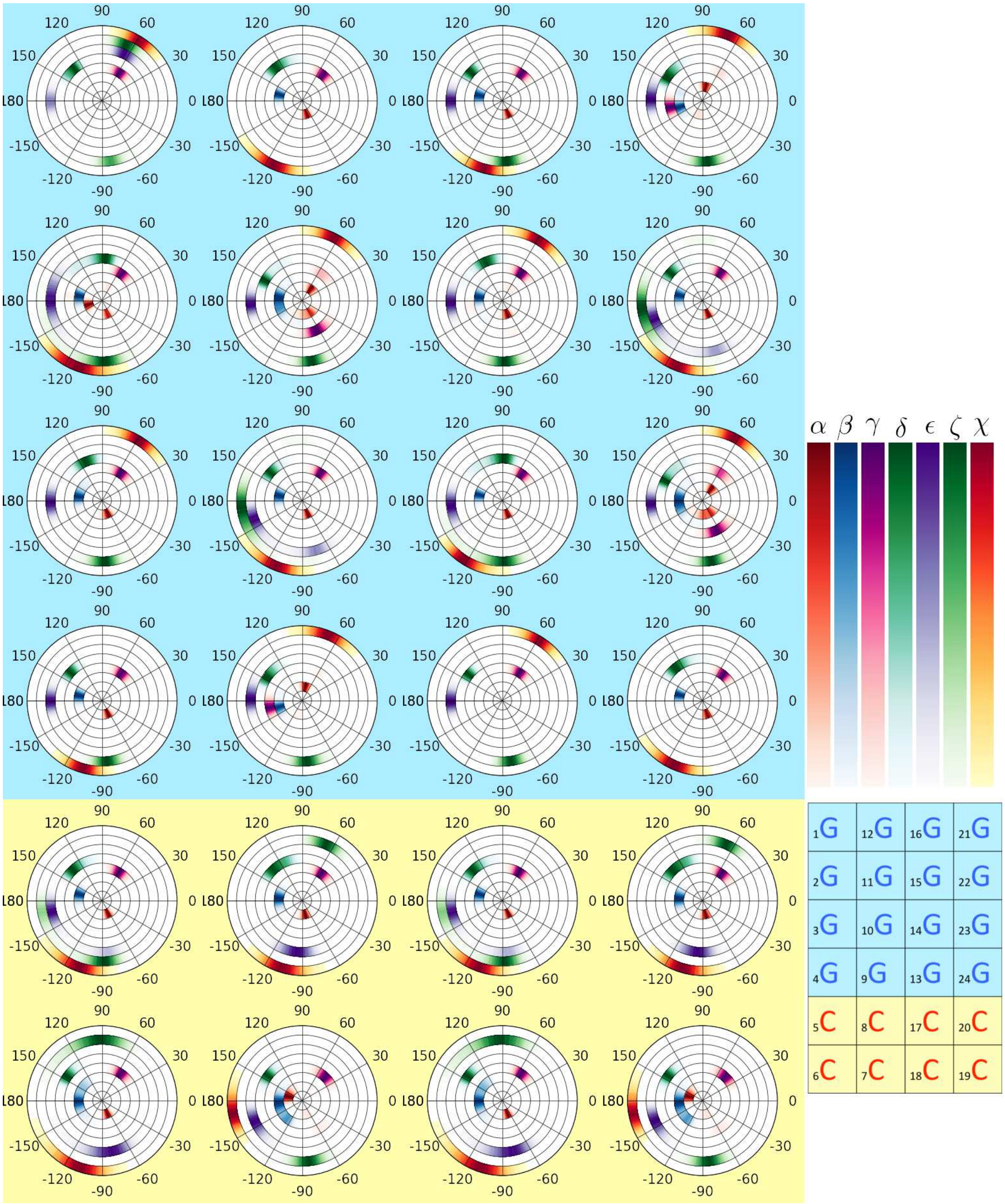

Figure S8: Torsion angle density distribution (α, β, γ, δ, ϵ, ζ, χ, from inner to outer circle ring) for each base in DNA AQ-1-L during the last 500 ns of the simulation. G-layers are shown in blue and C-layers in yellow. G bases on the same layer are shown in the same row, according to the map on the right.

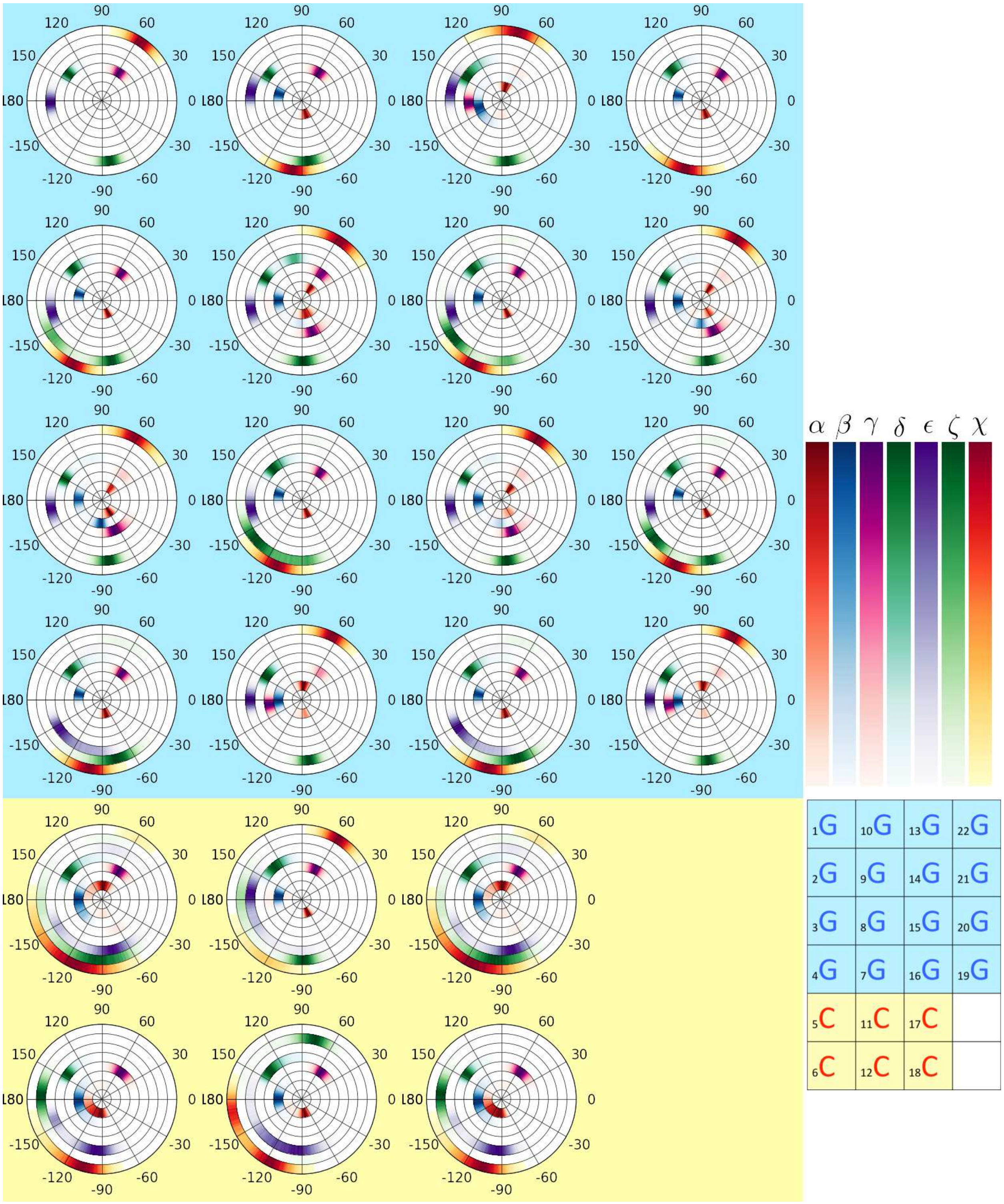

$_{1}$G	$_{10}$G	$_{13}$G	$_{22}$G
$_{2}$G	$_{9}$G	$_{14}$G	$_{21}$G
$_{3}$G	$_{8}$G	$_{15}$G	$_{20}$G
$_{4}$G	$_{7}$G	$_{16}$G	$_{19}$G
$_{5}$C	$_{11}$C	$_{17}$C	
$_{6}$C	$_{12}$C	$_{18}$C	

Figure S9: Torsion angle density distribution (α, β, γ, δ, ϵ, ζ, χ, from inner to outer circle ring) for each base in DNA AQ-2-L during the last 500 ns of the simulation. G-layers are shown in blue and C-layers in yellow. G bases on the same layer are shown in the same row, according to the map on the right.

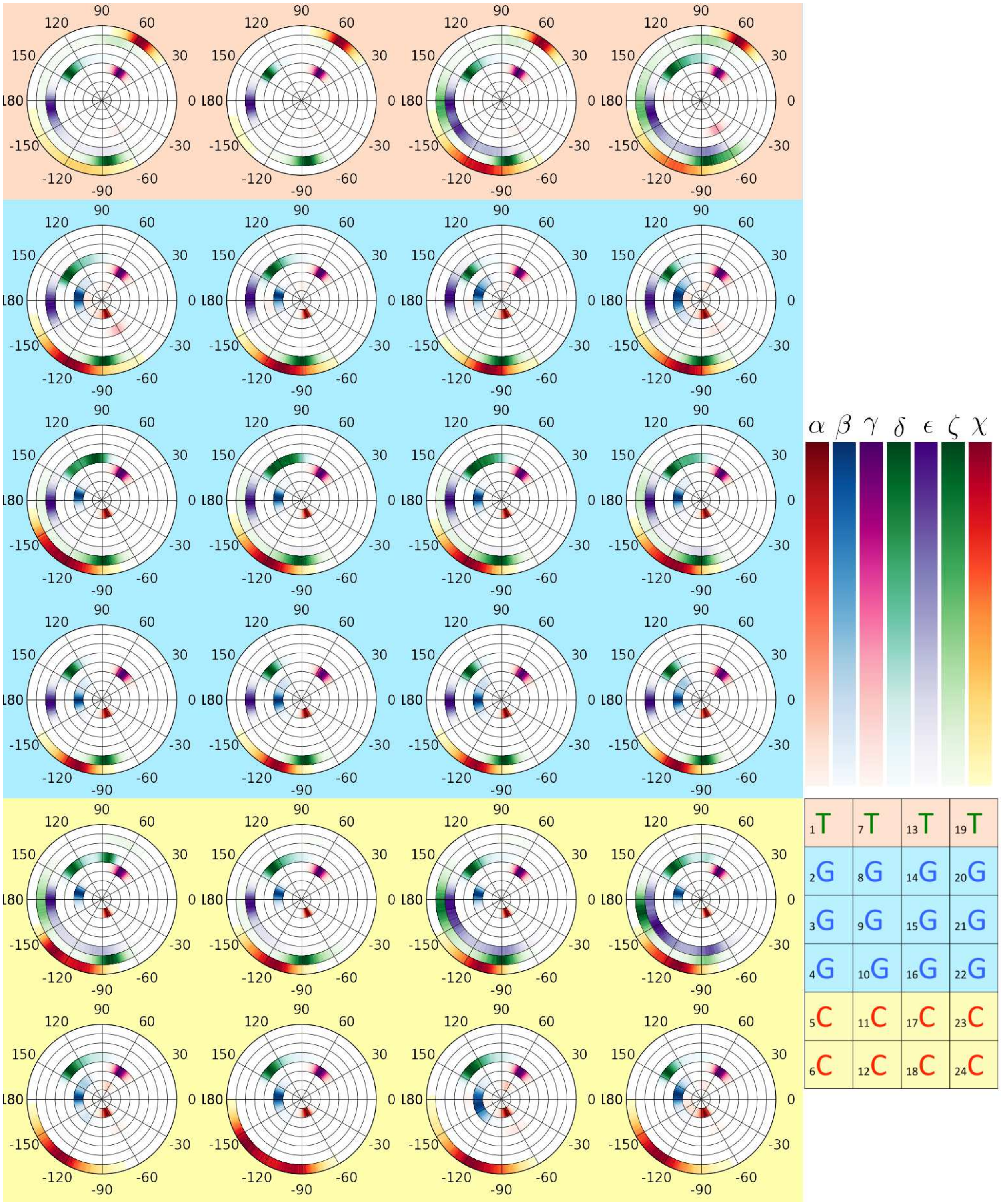

$_{1}$T	$_{7}$T	$_{13}$T	$_{19}$T
$_{2}$G	$_{8}$G	$_{14}$G	$_{20}$G
$_{3}$G	$_{9}$G	$_{15}$G	$_{21}$G
$_{4}$G	$_{10}$G	$_{16}$G	$_{22}$G
$_{5}$C	$_{11}$C	$_{17}$C	$_{23}$C
$_{6}$C	$_{12}$C	$_{18}$C	$_{24}$C

Figure S10: Torsion angle density distribution (α, β, γ, δ, ϵ, ζ, χ, from inner to outer circle ring) for each base in DNA SCA36-PQ during the last 500 ns of the simulation. G-layers are shown in blue, C-layers in yellow and T-layers in pink. G bases on the same layer are shown in the same row, according to the map on the right.

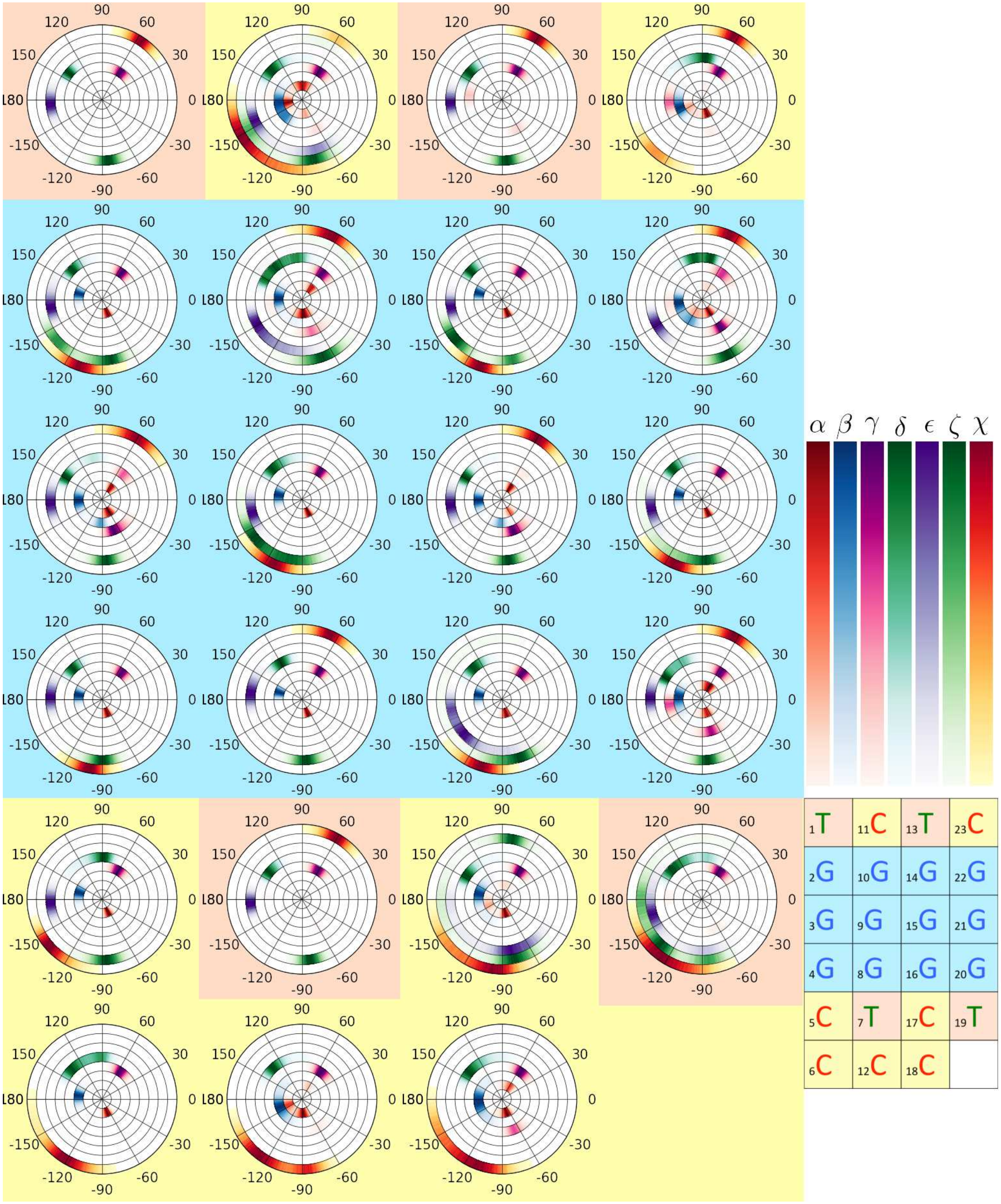

$_{1}$T	$_{11}$C	$_{13}$T	$_{23}$C
$_{2}$G	$_{10}$G	$_{14}$G	$_{22}$G
$_{3}$G	$_{9}$G	$_{15}$G	$_{21}$G
$_{4}$G	$_{8}$G	$_{16}$G	$_{20}$G
$_{5}$C	$_{7}$T	$_{17}$C	$_{19}$T
$_{6}$C	$_{12}$C	$_{18}$C	

Figure S11: Torsion angle density distribution (α, β, γ, δ, ϵ, ζ, χ, from inner to outer circle ring) for each base in DNA SCA36-AQ1 during the last 500 ns of the simulation. G-layers are shown in blue, C-layers in yellow and T-layers in pink. G bases on the same layer are shown in the same row, according to the map on the right.

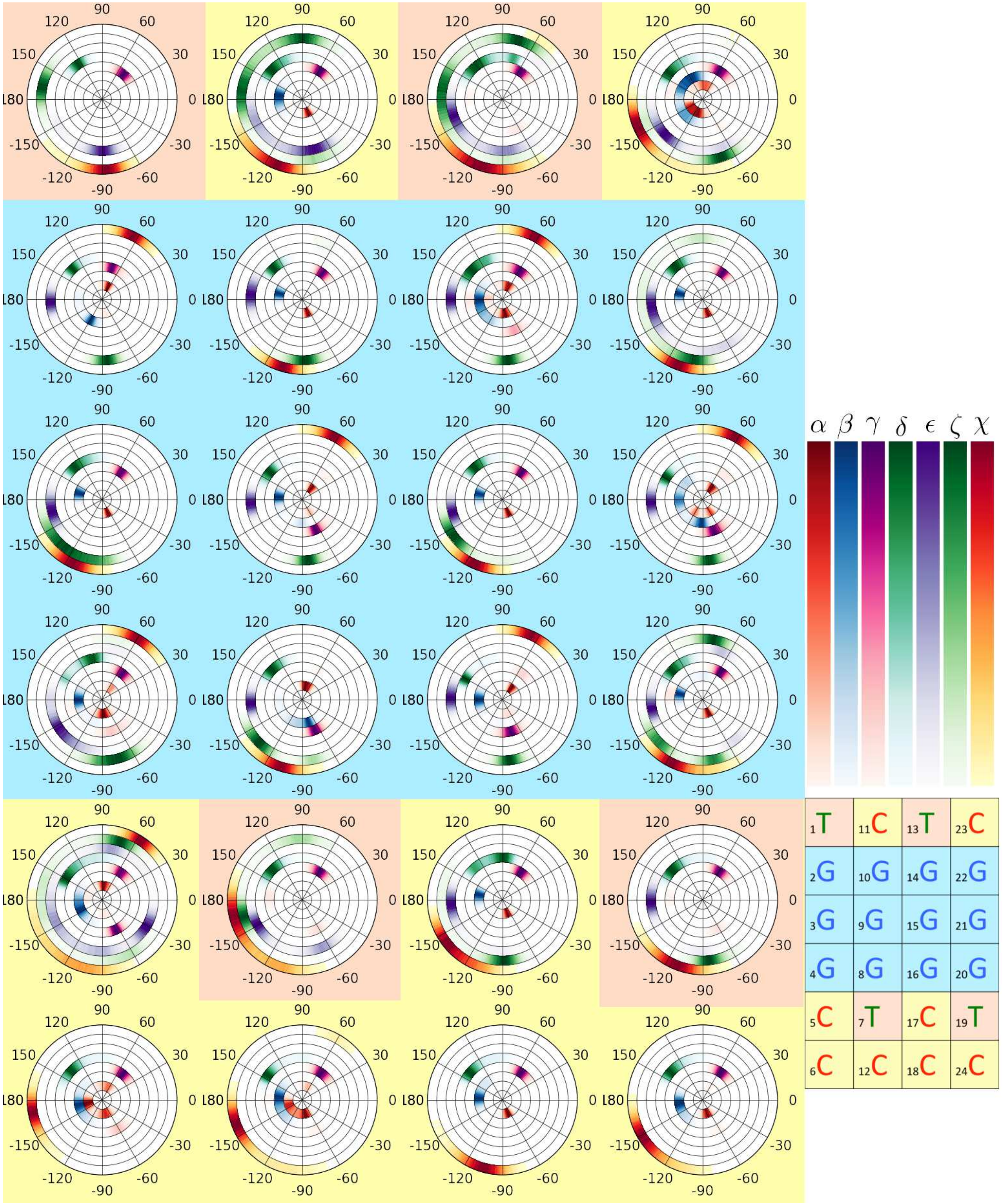

$_{1}$T	$_{11}$C	$_{13}$T	$_{23}$C
$_{2}$G	$_{10}$G	$_{14}$G	$_{22}$G
$_{3}$G	$_{9}$G	$_{15}$G	$_{21}$G
$_{4}$G	$_{8}$G	$_{16}$G	$_{20}$G
$_{5}$C	$_{7}$T	$_{17}$C	$_{19}$T
$_{6}$C	$_{12}$C	$_{18}$C	$_{24}$C

Figure S12: Torsion angle density distribution (α, β, γ, δ, ϵ, ζ, χ, from inner to outer circle ring) for each base in DNA SCA36-AQ2 during the last 500 ns of the simulation. G-layers are shown in blue, C-layers in yellow and T-layers in pink. G bases on the same layer are shown in the same row, according to the map on the right.

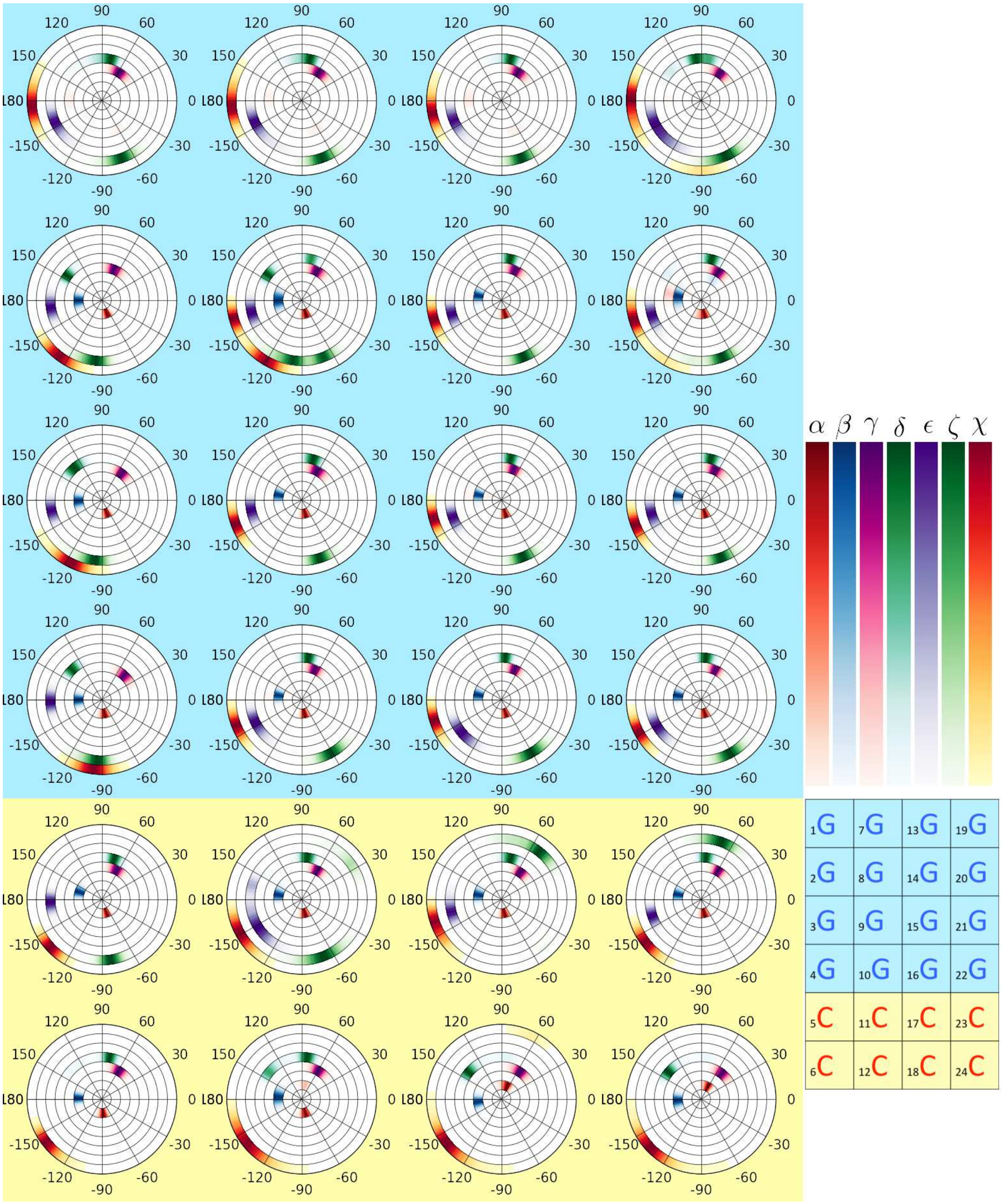

Figure S13: Torsion angle density distribution (α, β, γ, δ, ϵ, ζ, χ, from inner to outer circle ring) for each base in RNA PQ during the last 500 ns of the simulation. G-layers are shown in blue and C-layers in yellow. G bases on the same layer are shown in the same row, according to the map on the right.

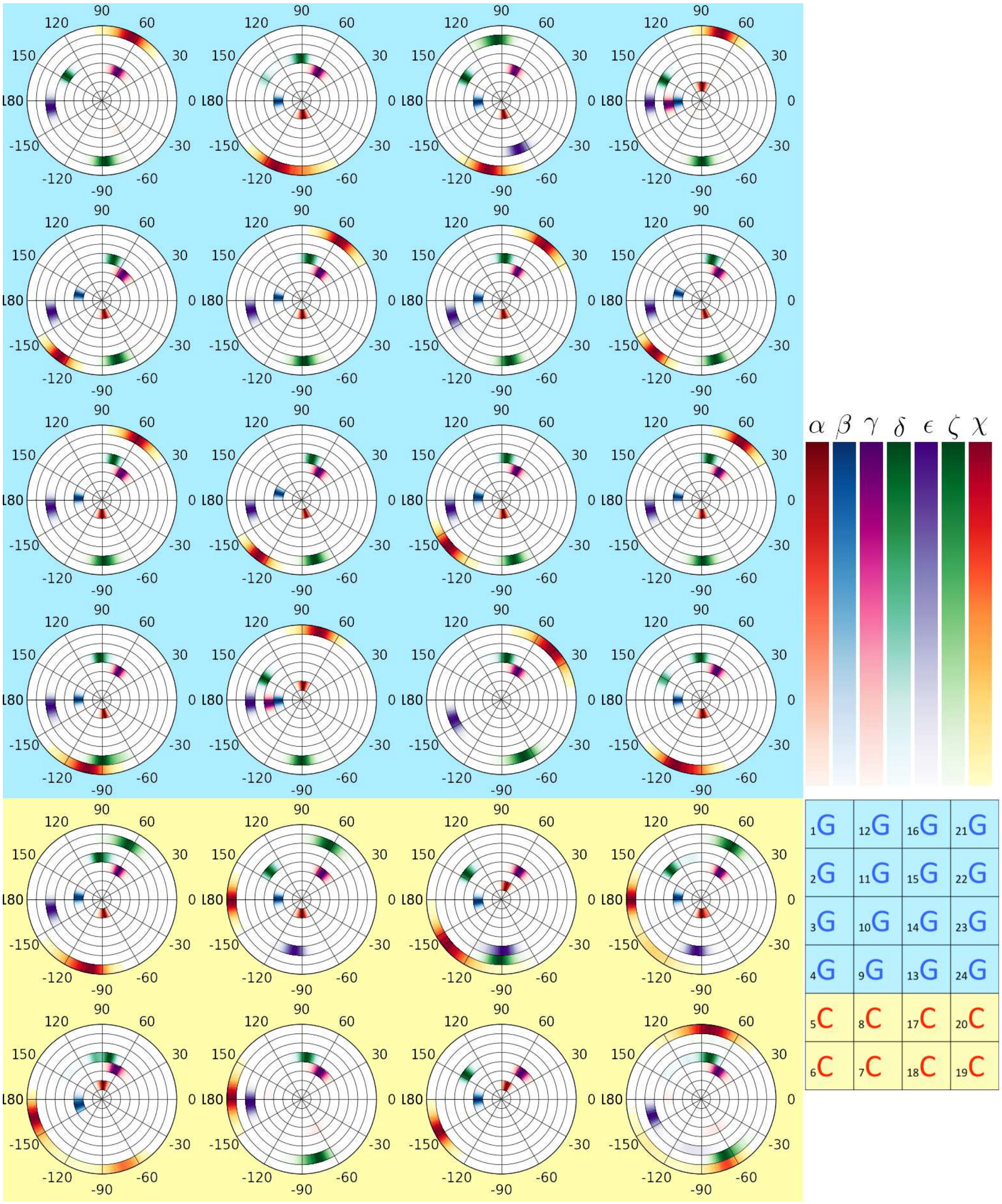

1G	12G	16G	21G
2G	11G	15G	22G
3G	10G	14G	23G
4G	9G	13G	24G
5C	8C	17C	20C
6C	7C	18C	19C

Figure S14: Torsion angle density distribution (α, β, γ, δ, ϵ, ζ, χ, from inner to outer circle ring) for each base in RNA AQ-1 during the last 500 ns of the simulation. G-layers are shown in blue and C-layers in yellow. G bases on the same layer are shown in the same row, according to the map on the right.

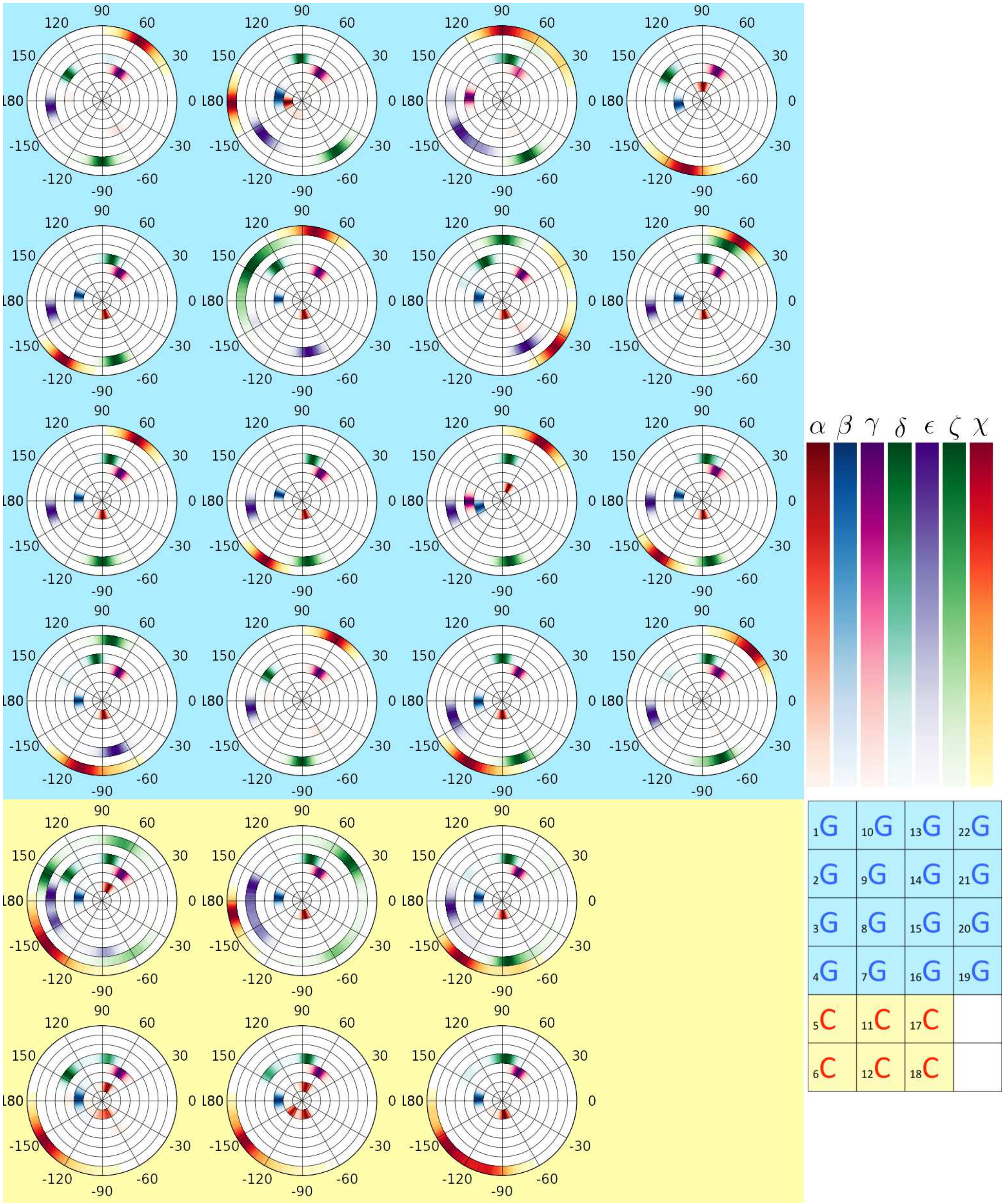

Figure S15: Torsion angle density distribution (α, β, γ, δ, ϵ, ζ, χ, from inner to outer circle ring) for each base in RNA AQ-2 during the last 500 ns of the simulation. G-layers are shown in blue and C-layers in yellow. G bases on the same layer are shown in the same row, according to the map on the right.

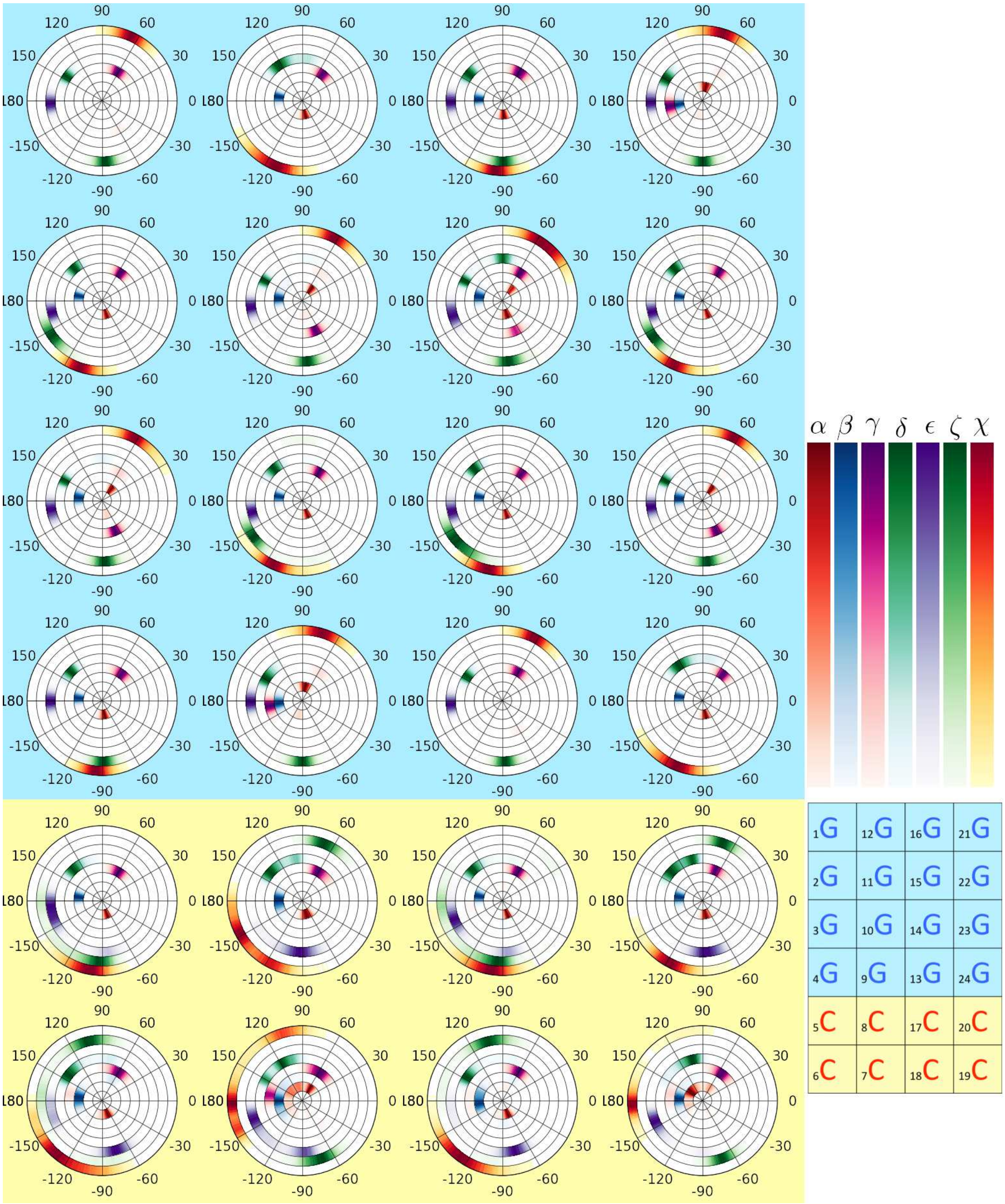

Figure S16: Torsion angle density distribution (α, β, γ, δ, ϵ, ζ, χ, from inner to outer circle ring) for each base in RNA AQ-1-L during the last 500 ns of the simulation. G-layers are shown in blue and C-layers in yellow. G bases on the same layer are shown in the same row, according to the map on the right.

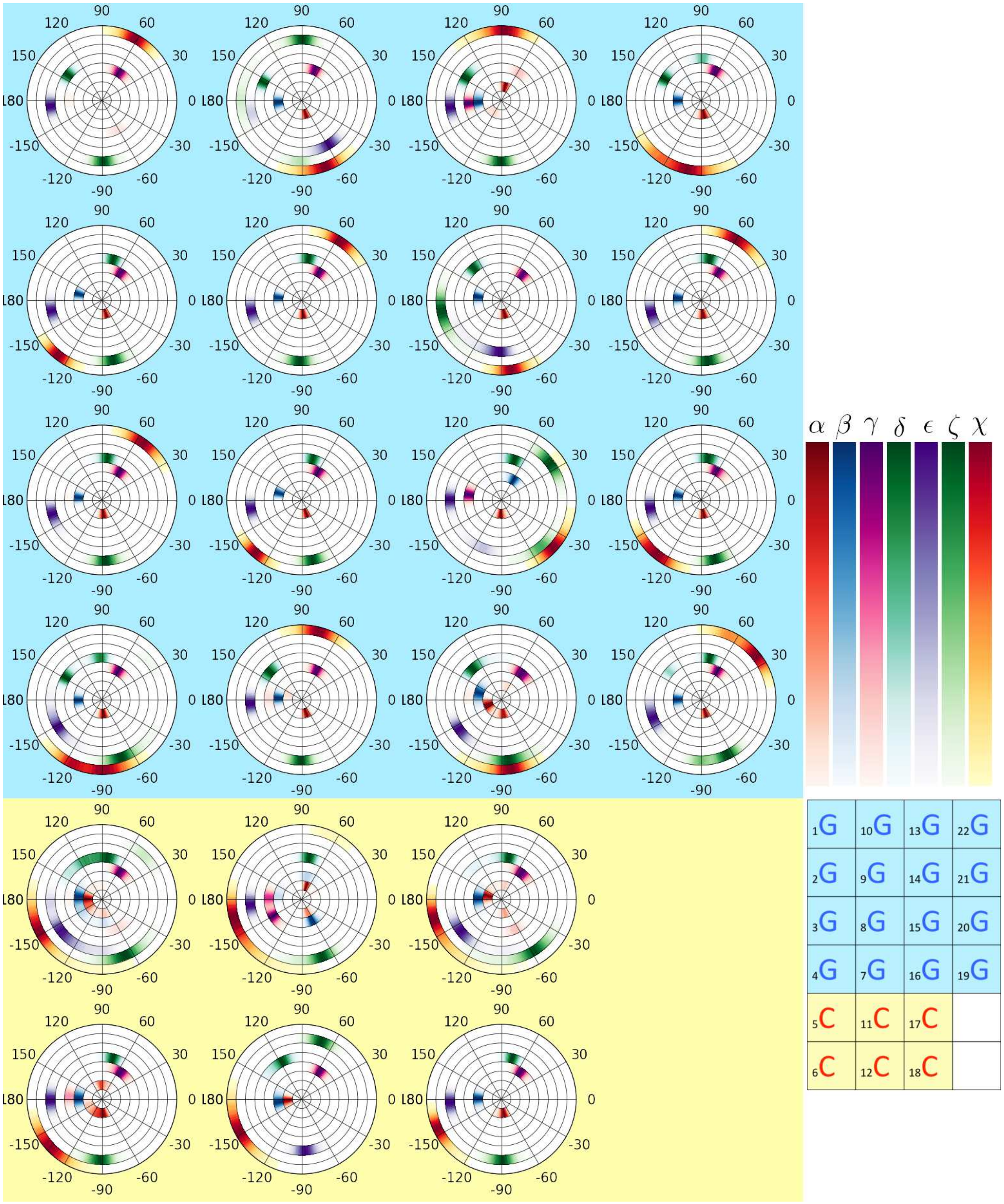

Figure S17: Torsion angle density distribution (α, β, γ, δ, ϵ, ζ, χ, from inner to outer circle ring) for each base in RNA AQ-2-L during the last 500 ns of the simulation. G-layers are shown in blue and C-layers in yellow. G bases on the same layer are shown in the same row, according to the map on the right.

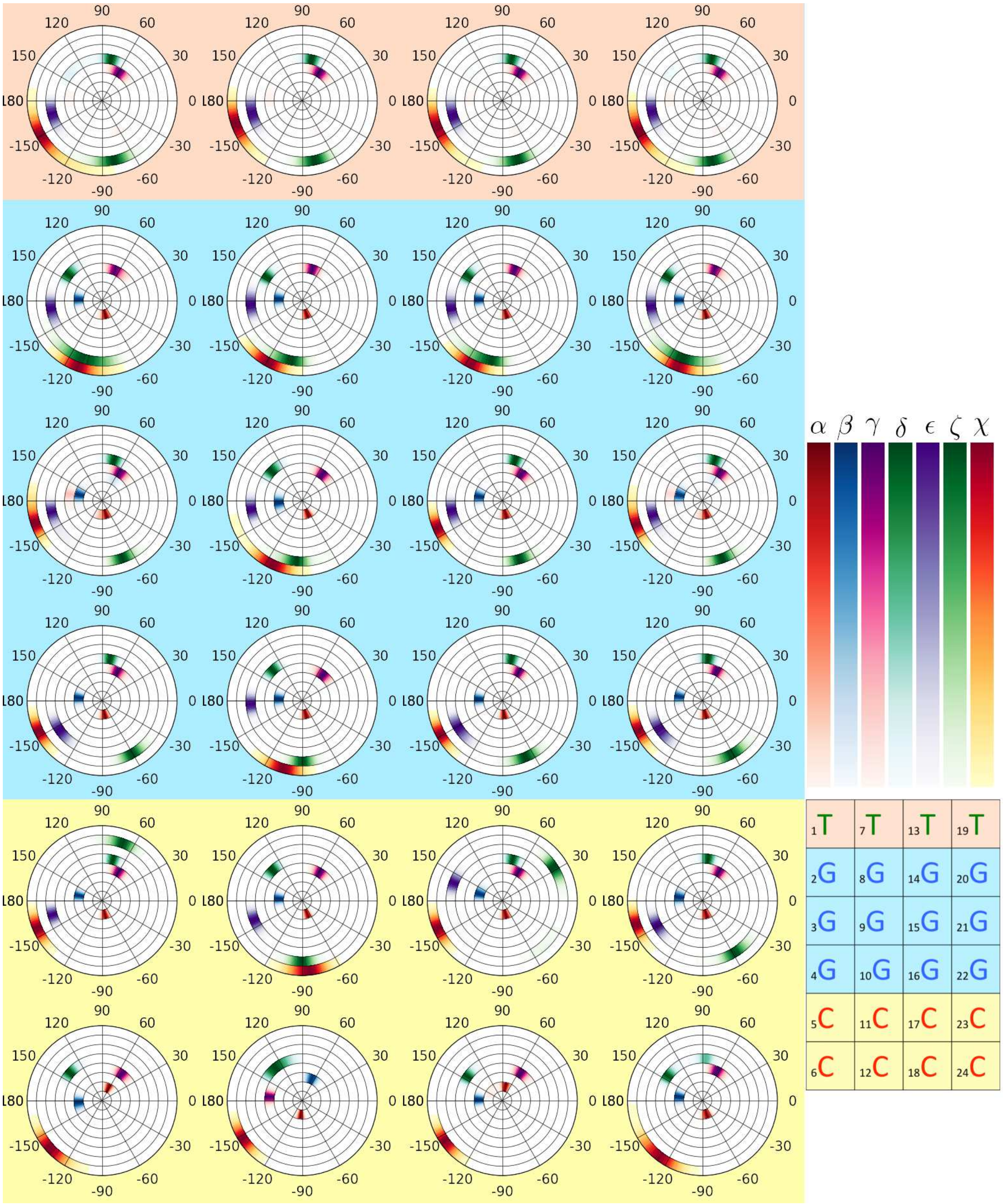

$_{1}$T	$_{7}$T	$_{13}$T	$_{19}$T
$_{2}$G	$_{8}$G	$_{14}$G	$_{20}$G
$_{3}$G	$_{9}$G	$_{15}$G	$_{21}$G
$_{4}$G	$_{10}$G	$_{16}$G	$_{22}$G
$_{5}$C	$_{11}$C	$_{17}$C	$_{23}$C
$_{6}$C	$_{12}$C	$_{18}$C	$_{24}$C

Figure S18: Torsion angle density distribution (α, β, γ, δ, ϵ, ζ, χ, from inner to outer circle ring) for each base in RNA SCA36-PQ during the last 500 ns of the simulation. G-layers are shown in blue, C-layers in yellow and T-layers in pink. G bases on the same layer are shown in the same row, according to the map on the right.

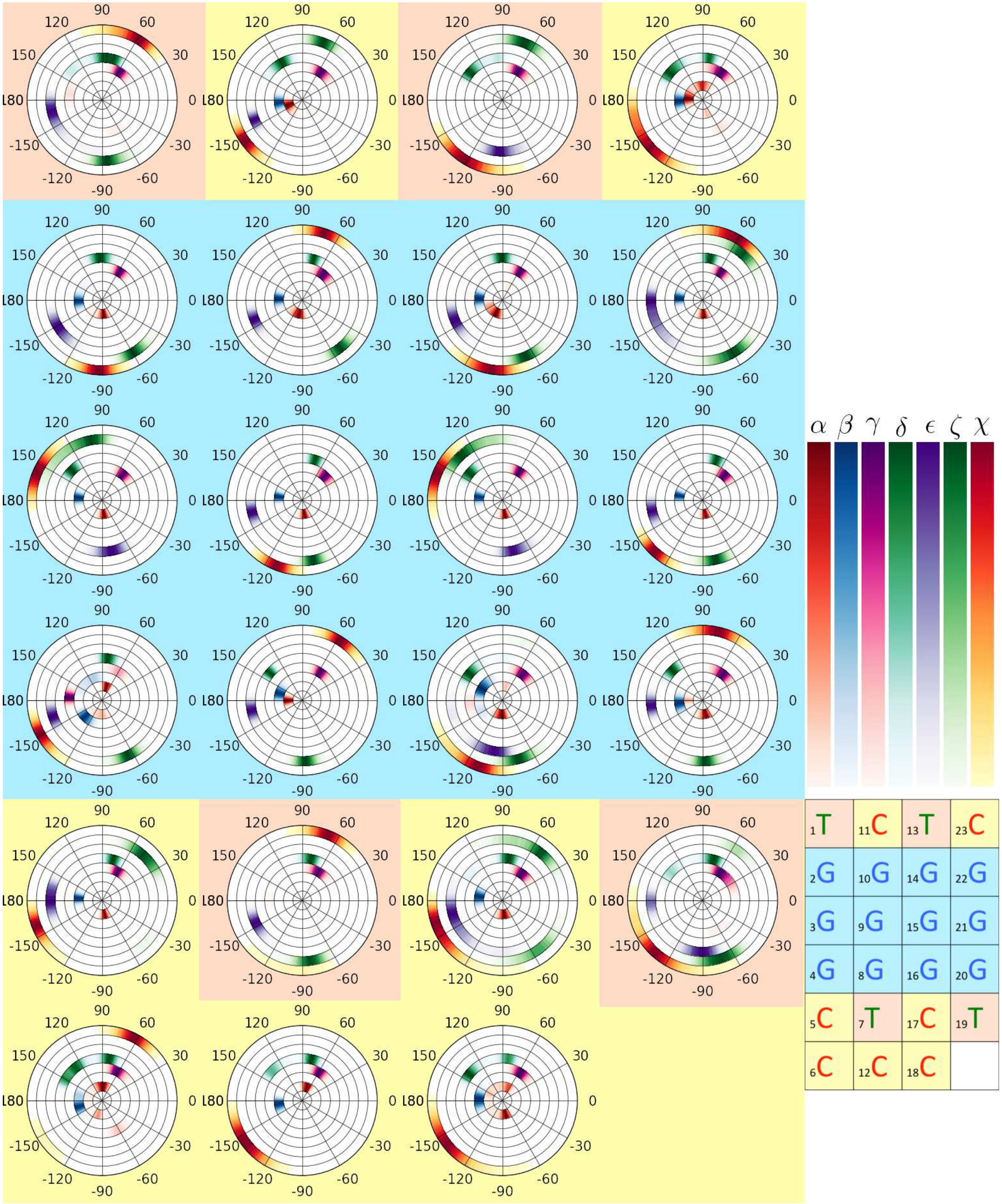

₁T	₁₁C	₁₃T	₂₃C
₂G	₁₀G	₁₄G	₂₂G
₃G	₉G	₁₅G	₂₁G
₄G	₈G	₁₆G	₂₀G
₅C	₇T	₁₇C	₁₉T
₆C	₁₂C	₁₈C	

Figure S19: Torsion angle density distribution (α, β, γ, δ, ϵ, ζ, χ, from inner to outer circle ring) for each base in RNA SCA36-AQ1 during the last 500 ns of the simulation. G-layers are shown in blue, C-layers in yellow and T-layers in pink. G bases on the same layer are shown in the same row, according to the map on the right.

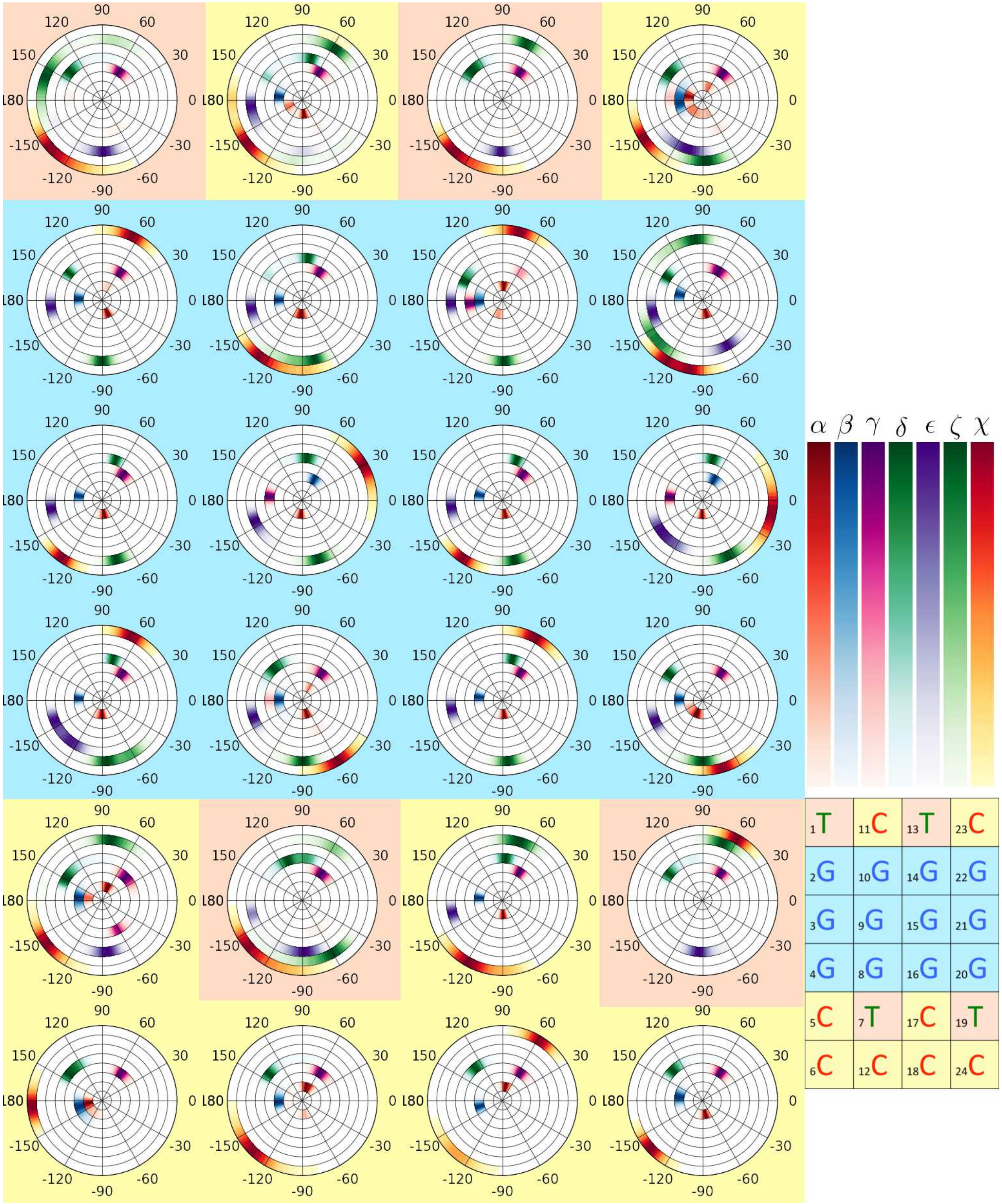

$_{1}$T	$_{11}$C	$_{13}$T	$_{23}$C
$_{2}$G	$_{10}$G	$_{14}$G	$_{22}$G
$_{3}$G	$_{9}$G	$_{15}$G	$_{21}$G
$_{4}$G	$_{8}$G	$_{16}$G	$_{20}$G
$_{5}$C	$_{7}$T	$_{17}$C	$_{19}$T
$_{6}$C	$_{12}$C	$_{18}$C	$_{24}$C

Figure S20: Torsion angle density distribution (α, β, γ, δ, ϵ, ζ, χ, from inner to outer circle ring) for each base in RNA SCA36-AQ2 during the last 500 ns of the simulation. G-layers are shown in blue, C-layers in yellow and T-layers in pink. G bases on the same layer are shown in the same row, according to the map on the right.